XV International Conference on Durability of Building Materials and Components
DBMC 2020, Barcelona
C. Serrat, J.R. Casas and V. Gibert (Eds)

Non-Destructive Evaluation of Micro-Cracked SCC by Ultrasonic Waves

Irene Palomar[1], Gonzalo Barluenga[1], Hugo Varela[1], Javier Puentes[2] and Ángel Rodríguez[3]

[1] Department of Architecture, University of Alcala, Madrid, Spain, irene.palomar@uah.es; gonzalo.barluenga@uah.es; hugo.varela@edu.uah.es

[2] Institute of Construction Sciences Eduardo Torroja, CSIC, Spain, javier.puentes@ietcc.csic.es

[3] Systems Engineering and Automation Dept., University Carlos III of Madrid, Spain, angrodri@ing.uc3m.es

Abstract. *Self-Compacting Concrete (SCC) is an effective, reliable and safer technology to cast-in-place concrete structures. However, the large amount of paste required to achieve its high flowability may increase drying shrinkage at early age, due to the undesirable effects of curing conditions, producing micro-cracking and damaging concrete members. When this happens, an evaluation of the hardened SCC is necessary and Non-destructive testing techniques (NDT) can be suitable. Among NDT, Ultrasonic pulses (US) have showed to be very useful due to its portability, easiness of application and sensitivity to changes in material microstructure, porosity and presence of defects. In order to evaluate the applicability of ultrasonic (US) waves to better understand the relations among composition, microstructure, properties, curing conditions and micro-cracking, an experimental program using transmission P- and S- waves was carried out on SCC with limestone filler (LF), microsilica (MS) and nanosilica (NS), set and hardened under different curing conditions: 10, 20 and 30 °C and 40 and 80 % relative humidity. Free shrinkage and double displacement restrained slabs were tested and cracking potential due to Early Age Shrinkage was assessed. Ultrasonic transmission time and wave amplitude of the raw US signal were measured and Ultrasonic pulse velocity (UPV) and attenuation coefficient were calculated. In addition, some physical and mechanical properties of cracked and un-cracked samples were measured. The aim of this study was to compare US parameters to hardened properties of cracked and un-cracked SCC. Correlations for SCC micro-cracking based on US parameters were identified, demonstrating the potential of using transmission US P- and S- waves as an evaluation technique for micro-damaged SCC.*

Keywords: *Ultrasonic, P and S Waves, Micro-Cracking, SCC, Hardened Properties.*

1 Introduction

Self-Compacting Concrete (SCC) is designed to improve cast-in-place structures by increasing paste phase and enhancing fresh rheology. However, larger paste volume makes SCC more sensitive to curing conditions, increasing early age (EA) drying shrinkage and micro-cracking potential (Puentes *et al.*, 2014). SCC usually incorporates supplementary cementitious materials (SCM) in its composition. The type and amount of SCM used has been identified to also affect cracking potential damage jointly with curing conditions on SCC with limestone filler, microsilica and nanosilica (Barluenga *et al.*, 2018). When EA cracking occurs, an evaluation of the hardened properties of SCC is necessary. Among the Non-destructive testing techniques (NDT) available, radar, electrical resistivity, capacitance measurements and ultrasound have been described to be suitable for estimating material properties (Garnier *et al.*, 2013). Ultrasonic

pulses (US) is often preferred due to its portability, easiness of application and sensitivity to changes in material microstructure, porosity and defect detection (Selleck *et al.*, 1998; Aggelis, 2013; Barluenga *et al.*, 2015; Palomar *et al.*, 2017). US parameters such as ultrasonic transmission times and wave amplitude of the raw US signal propagated through the material can be used to evaluate the relations among composition, microstructure, properties, curing conditions and micro-cracking (Yim *et al.*, 2012; Shiotani *et al.*, 2009). The most commonly used US wave type is compressive or P-wave, although there are transducers commercially available that combine P- and S-waves (shear pulses). Thus, the wave velocity propagation (UPV), the wave attenuation coefficient (AT) and Young modulus, Shear modulus and Poisson's coefficient ratio can be calculated (Palomar *et al.*, 2017). The combination of US parameters considering both UPV and AT can be used for concrete micro-cracking assessment (Shiotani *et al.*, 2009).

The aim of this study was to compare US parameters to hardened properties of cracked and un-cracked SCC with limestone filler (LF), microsilica (MS) and nanosilica (NS). An experimental program using transmission P- and S- waves was carried out on SCC set and hardened under different curing conditions. The applicability of ultrasonic (US) waves to better understand the relations among composition, microstructure, properties, curing conditions and micro-cracking was evaluated.

2 Experimental Program

2.1 Materials and Mixtures

SCC mixtures are summarized in Table 1. A reference SCC containing a CEM I 42.5 R cement, limestone filler; fine and coarse aggregates, water and 1% by weight of cement (bwoc) of a high range water reducing admixture (HRWRA) was designed (HCA). Afterwards, limestone filler was replaced by densified microsilica (HCAMS) and colloidal nanosilica (HCANS), 10 and 5% bwoc respectively (see Barluenga *et al.*, 2018 for further descriptions).

2.2 Experimental Methods and Preliminary Results

2.2.1 Early age cracking potential in different curing conditions

Early age (EA) cracking potential was measured using a double restrained slab test subjected to 10, 20 and 30 ℃ curing temperatures and 40 and 80 % relative humidity (RH) during the first 24 h. The test setup consisted of 400 x 300 x 45 mm slabs, with double displacement restricted by internal plugs attached to the mold, in order to maximize EA cracking potential (Barluenga *et al.*, 2018). The slabs were demolded at 24 h and stored in laboratory conditions until crack measurement at 7 days. The cracked area (A_c) summarized in Table 2 was calculated measuring cracks length (L) and width (W) (Puentes *et al.*, 2014). The results of the SCC mixes with filler (HCA) showed high A_c. It can also be observed that the L and W for HCA were higher, especially at 20℃ and 40% RH. SCC with Microsilica (HCAMS) reduced significantly EA cracking, except for hot-dry conditions. In the case of SCC with nanosilica (HCANS) A_c was slightly lower, although the cracks were narrower than HCA and HCAMS. In general, silica based additions at hot-dry conditions showed a high EA cracking risk, whereas it was minimized

in hot-wet conditions. The increase of hydration speed and microstructure formation in hot-dry curing conditions may explain this effect on EA cracking (Barluenga *et al.*, 2018).

Table 1. SCC Compositions (kg/m^3).

	HCA	**HCAMS**	**HCANS**
Cement	350	350	350
Limestone Filler	350	315	332.5
Gravel (4–20 mm)	790	790	790
Sand (0–4 mm)	679	679	679
Microsilica	-	35	-
Nanosilica	-	-	79.5
Water*	179	179	117
HRWRA	3.5	3.5	3.5
w/c **	0.6	0.6	0.6
w/b **	0.3	0.3	0.3

* Liquid water added.
** The amount of water included in the components (sand humidity (4.3%), SP and NS) was also considered.

Table 2. Early age cracking parameters. Physical and mechanical properties at hardened state.

	A_c mm^2/m^2	**L_{max}** mm	**W_m** mm	**AER*** 10^3ml/s mm^2	**WAR *** 10^6ml/s mm^2	**Po**** %	**CS**** MPa
HCA	539	66	0.17	0.48	0.93	2.34	34
10-40	353	70	0.07	0.63	1.12	2.55	35
10-80	448	90	0.18	0.27	1.09	3.11	30
20-40	2139	145	0.66	0.45	1.25	1.85	35
20-80	0	0	0	0.73	1.29	3.21	31
30-40	42	25	0.05	0.67	0.32	-	34
30-80	253	65	0.06	0.13	0.50	0.97	37
HCAMS	122	17	0.05	0.18	1.02	1.88	33
10-40	91	25	0.09	0.18	1.03	2.47	37
10-80	0	0	0	0.12	1.52	1.28	36
20-40	0	0	0	0.09	0.67	2.22	32
20-80	0	0	0	0.17	0.83	2.33	37
30-40	641	75	0.21	0.47	1.37	2.06	29
30-80	0	0	0	0.07	0.67	0.92	30
HCANS	327	59	0.06	0.22	1.05	2.29	36
10-40	166	70	0.06	0.16	2.18	1.98	42
10-80	231	50	0.05	0.31	1.09	2.58	37
20-40	391	140	0.12	0.10	0.51	1.43	34
20-80	592	55	0.05	0.17	0.94	2.21	36
30-40	584	40	0.06	0.25	0.70	4.64	33
30-80	0	0	0	0.32	0.87	0.89	36

***** Cracked samples. ** Un-cracked samples at 28 days.

2.2.2 NDT assessment by ultrasonic pulse propagation

Ultrasonic pulses (US) were applied on hardened samples of cracked and un-cracked SCC samples with dimensions of 400 x 300 x 45 mm and 60 x 50 x 100 mm, respectively. P- and S-

waves 250 kHz transducers were used. The amplitude (V) in time domain (μs) of the P- and S-wave raw signal through SCC samples were obtained. P-wave (Pw) and S-wave (Sw) pulse velocity were identified using the Hilbert transform algorithm (Birgül, 2009). In addition, attenuation coefficient (AT_{250}) was calculated (Palomar *et al.*, 2017), where the higher AT_{250}, the lower the US energy absorbed by the SCC sample.

2.2.3 SCC hardened properties

Table 2 also summarizes several hardened physical and mechanical properties measured on 400 x 300 x 45 mm cracked slabs or 100 x 100 x 100 mm un-cracked samples. Air and water permeability were measured on cracked SCC slabs with a Figg's method based apparatus (Porosiscope™). The measured time for air or water to permeate through the concrete was used to estimate Air Exclusion Rating (AER) and Water Absorption Rate (WAR), respectively (Barluenga *et al.*, 2017). Open porosity accessible to water (P_O) and compressive strength (CS) were measured on cubic un-cracked samples at 28 days. HCA showed higher air permeability than SCC with silica based additions, while water permeability values were similar for all SCC compositions. Regarding curing conditions, HCA and HCANS samples showed large AER values even when cracks were not observed on the slabs. In contrast, the most damaged HCAMS slab presented the highest AER value. WAR was larger for HCA and HCAMS slabs without visible damage. SCC with nanosilica (HCANS) produced large values of WAR at cold-dry conditions despite its higher CS. Some correlations among the composition parameters, hardened properties and curing conditions have been described in a previous work (Barluenga *et al.*, 2018). Regarding SCC compositions, HCAMS reduced open porosity and HCANS increased compressive strength. In general, hot-wet curing conditions produced lower P_O, independently to the SCC composition, and increased CS on HCA samples. Cold-dry environment on HCMS and HCANS produced higher CS.

Table 3. P- and S-wave velocity and attenuation coefficient of US signal for SCC un-cracked samples.

	Pw m/s	**Sw** m/s	**AT_{250}** dB/mm
HCA	3938	2472	0.36
HCAMS	3926	2342	0.53
HCANS	3684	2201	0.52

3 Experimental Results and Discussion

3.1 Ultrasonic Characterization of Un-Cracked SCC Samples

Table 3 summarizes the experimental results of P- and S-wave propagation velocities (Pw and Sw) and attenuation coefficient (AT_{250}) of un-cracked SCC samples. Pw and AT_{250} presented lower variability related to SCC compositions. In contrast, Sw was sensitive to SCC composition: the smaller the particle size, the slower S-wave propagation velocity. Figure 1 plots the experimental results of Pw and Sw and AT_{250} of un-cracked SCC samples in different curing conditions. Pw and AT250 presented a high variability, although they showed different trends, while Sw did not depend on curing conditions.

3.2 Ultrasonic Evaluation of Cracked SCC Samples

Figure 2 and 3 plot the experimental results of Pw and Sw and AT_{250} of cracked SCC samples.

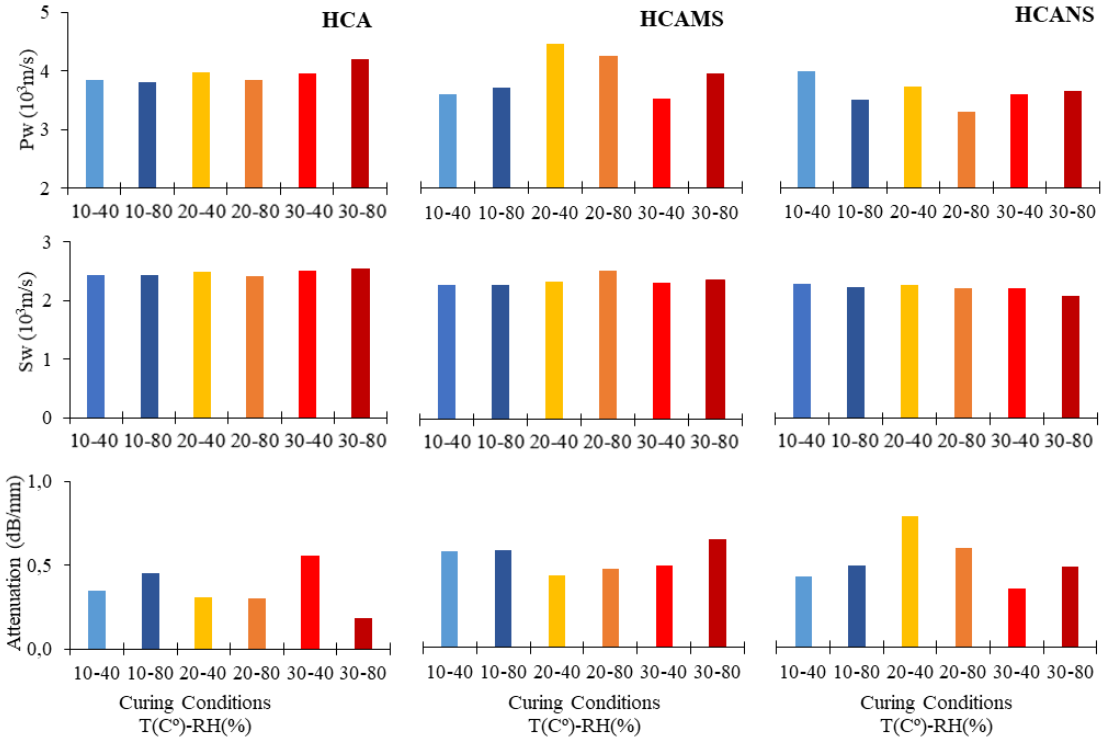

Figure 1. P- and S-wave velocity and attenuation coefficient of US signal for SCC un-cracked samples at different curing conditions.

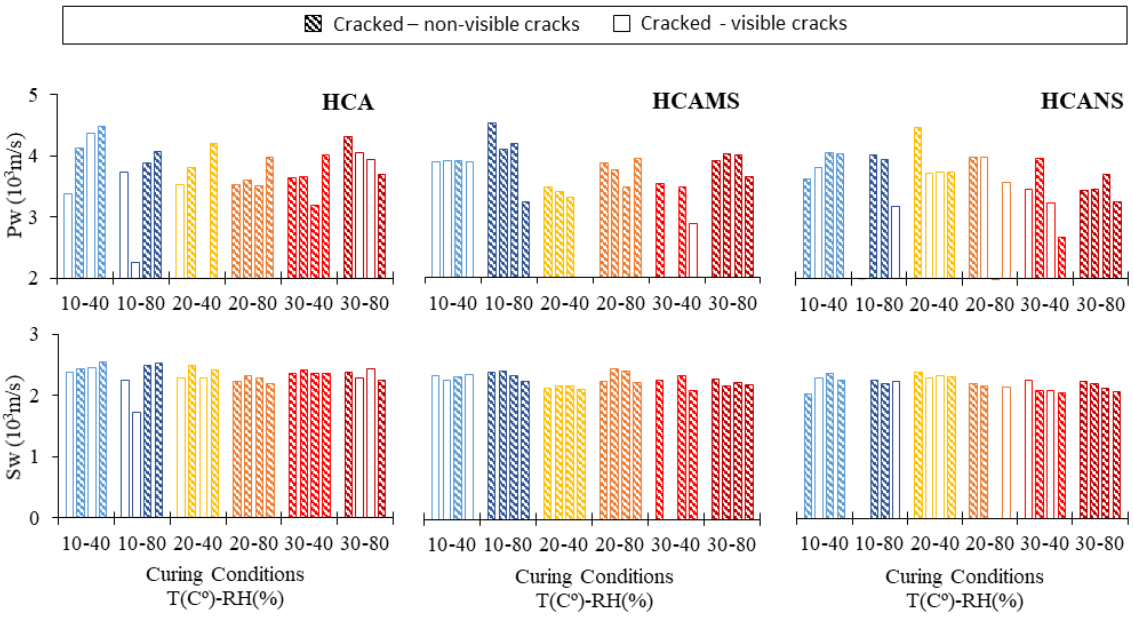

Figure 2. P- and S-wave velocity of US signal for SCC cracked samples at different curing conditions.

US propagation was measured on damaged slabs with visible (VC) and non-visible cracks (NVC). Regarding US velocities, Pw scatter was slightly higher in cracked samples than in un-cracked samples, although cracked values were lower than un-cracked. Pw on NVC was around 230 m/s faster than VC. Sw showed very low variability on cracked samples despite the effect of composition, curing conditions and NVC or VC. In addition, some damaged samples showed similar Pw and Sw values, with differences smaller than 1000 m/s. These values do not correspond to undamaged SCC and cannot be used to calculate mechanical properties of damaged slabs, as elastic modulus or Poisson Coefficient (Barluenga *et al.*, 2018).

A large dispersion of attenuation was recorded for cracked samples (Figure 3) and AT_{250} was higher for VC than NVC. The highest AT_{250} values (closely 1.00 dB/mm) corresponded to the widest cracks measured (HCA-1080 and 2040 and HCAMS-3040). Thus, cracks decreased the amplitude of the wave in damaged areas due to scattering and diffraction effects (Yim *et al.*, 2012). These results points out the sensitivity of AT_{250} to concentrated damage as visible cracks. However, some cracks produced by EA shrinkage of displacement restrained SCC members can progress from inside of the sample (Serpukhov *et al.*, 2010), producing AT_{250} values with little differences between VC and NVC areas. Accordingly, AT_{250} can detect both VC and NVC.

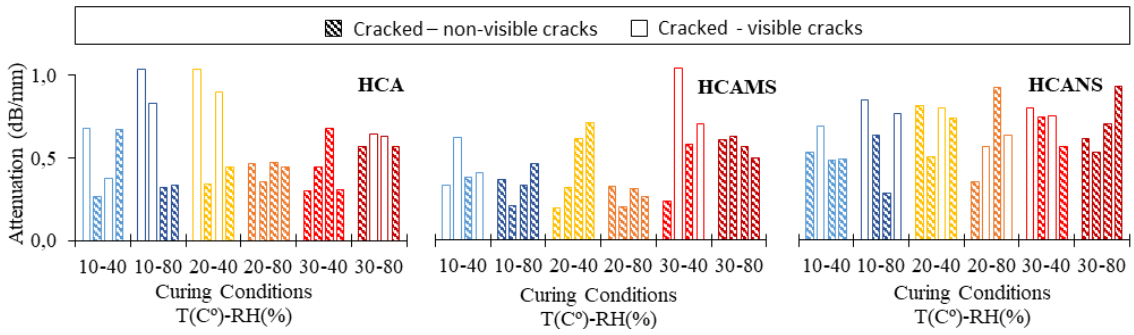

Figure 3. Attenuation coefficient of US signal for SCC cracked samples at different curing conditions.

3.3 Damage Evaluation of SCC Using NDT

An evaluation of damage and cracking potential by US analysis was carried out and is plotted in Figures 4 and 5, respectively. Regarding damage and US parameters, in general velocities of cracked samples were slower than on un-cracked samples (Selleck *et al.*, 1998), except HCA and HCAMS cured at 10º C. On the other hand, two behaviors were identified in AT_{250}: 1) HCA and HCANS; values of un-cracked samples were lower than cracked ones; 2) HCAMS AT_{250} values were higher for un-cracked than for cracked samples. These differences can be explained considering the effect of SCC composition on cracking potential. HCA and HCANS showed larger cracking potential, whereas HCAMS cracking potential was remarkably lower. There were two exceptions to this trends: HCAMS 3040 (visible damage) and HCANS-2040 (red labeled in the graph). This last case showed long and wide cracks and low AER and WAR, meaning concentrated damages that can explain its exceptionality.

As a predictive tool for EA cracking potential of SCC, cracked area (A_c) can be compared to the ratio between Pw and Sw (Pw/Sw) of un-cracked samples (Figure 5). The results showed an inverse relationship between Pw/Sw and A_c until a constant value of 1.60 or 1.80, which

depended on sample composition. A ratio of 1.80 means a Poisson's ratio (υ) around 0.28: the larger the ratio the lower the compressibility. Therefore, if the un-cracked sample reaches a certain Pw/Sw or compressibility, EA cracking potential will be minimized (HCAMS and HCANS). In the case of HCA, Pw/Sw showed littele cracking potential variability.

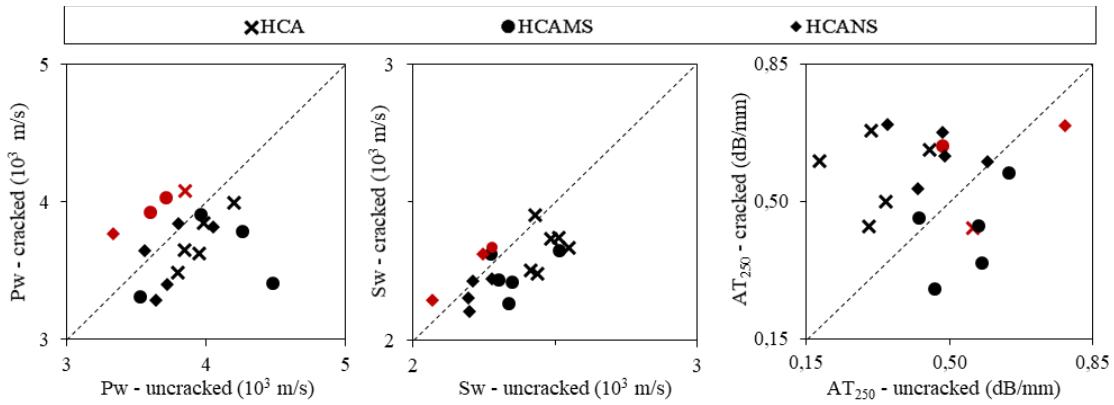

Figure 4. Ultrasonic pulse velocity and attenuation coefficient: un-cracked vs cracked values.

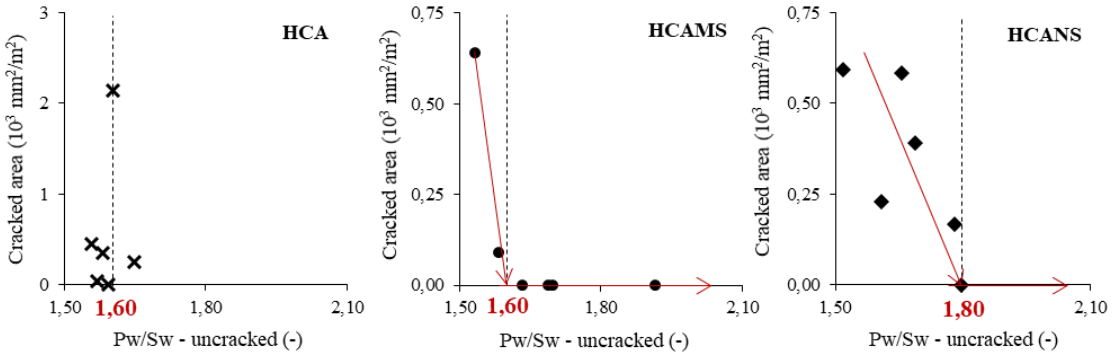

Figure 5. P- and S-wave velocity ratio (Pw/Sw) for un-cracked samples vs EA cracking parameters (A_c).

4 Conclusions

The applicability of ultrasonic (US) waves to better understand the relations among composition, microstructure, properties, curing conditions and early age cracking potential of SCC with limestone filler (LF), microsilica (MS) and nanosilica (NS) was assessed. The influence of composition, curing conditions and micro-damage on US parameters (P- and S-wave velocities and signal attenuation) were analyzed. The main conclusions were:

- Changes in SCC compositions and curing conditions modified early age (EA) cracking potential and hardened properties.
- SCC compositions and curing conditions had a significant effect on US velocity propagation and attenuation coefficient in un-cracked and cracked samples, although the effect on US parameters it is not linear.
- US parameters were identified as key parameters to assess the micro-damage or the EA cracking potential of SCC.
- US velocities of un-cracked samples were higher than those of cracked samples. The

attenuation coefficient of un-cracked SCC was lower than the damaged samples, either when the cracks were externally visible and when they were internal and non-visible.
- EA cracking potential was estimated for samples set and hardened under same curing conditions, using P- and S-wave velocity ratio (Pw/Sw) of un-cracked samples.

Acknowledgements

Financial support was provided by the Spanish Ministry of Economy & Competitiveness (NanoCompaC, BIA2016-77911-R) and UAH (postdoctoral fellowship - Ayuda Postdoctoral/Modalidad A/2017). Some of the components were supplied by BASF Spain S.L, Omya Clariana S.L, and Portland Cement Vaderrivas.

ORCID

Irene Palomar: https://orcid.org/0000-0003-2743-3618
Gonzalo Barluenga: https://orcid.org/0000-0002-2996-3412
Hugo Varela: https://orcid.org/0000-0001-8094-6071
Javier Puentes: https://orcid.org/0000-0001-8748-7664
Ángel Rodríguez: http://orcid.org/0000-0002-6897-2194

References

Aggelis, D.G. (2013). Wave propagation through engineering materials; assessment and monitoring of structures through non-destructive techniques. *Materials and Structures, 46*, 519-532. doi: 10.1617/s11527-013-0020-x

Barluenga, G., Guardia, C. and Puentes, J. (2018). Effect of curing temperature and relative humidity on early age and hardened properties of SCC. *Construction and Building Materials, 167*, 235-242. doi: 10.1016/j.conbuildmat.2018.02.029

Barluenga, G., Guardia, C. and Puentes, J. (2017). Effect of curing conditions on microstructure, cracking and durability of SCC. In *Proceedings of the 14th International Conference on Durability of Building Materials and Components (RILEM PRO 107)*, Ghent, Bélgica, 163 (DBMC-p163.pdf).

Barluenga, G., Palomar, I. and Puentes, J. (2015). Hardened properties and microstructure of SCC with mineral additions. *Construction and Building Materials, 94*, 728-736. doi: 10.1016/j.conbuildmat.2015.07.072

Birgül, R. (2009). Hilbert transformation of waveforms to determine shear wave velocity in concrete. *Cement and Concrete Research, 39(8)*, 696-700. doi: 10.1016/j.cemconres.2009.05.003

Garnier, V., Piwakowski, B., Abraham, O., Villain, G., Payan, C. and Chaix, J.F. (2013). Acoustic techniques for concrete evaluation: Improvements, comparisons and consistency. *Construction and Building Materials, 43*, 598-613. doi: 10.1016/j.conbuildmat.2013.01.035

Palomar, I. and Barluenga, G. (2017). Assessment of lime-cement mortar microstructure and properties by P- and S- ultrasonic waves. *Construction and Building Materials, 139*, 334-341. doi: 10.1016/j.conbuildmat.2017.02.083

Puentes, J., Barluenga, G. and Palomar, I. (2014). Effects of nano-components on early age cracking of self-compacting concretes. *Construction and Building Materials, 73*, 89-96. doi: 10.1016/j.conbuildmat.2014.09.061

Selleck, S.F., Landis, E.N., Peterson, M.L., Shah, S.P. and Achenbach, J.D. (1998). Ultrasonic Investigation of Concrete with Distributed Damage. *ACI Materials Journal, 95-M4*, 27-36.

Serpukhov, I. and Mechtcherine, V. (2015). Early-age shrinkage of ordinary concrete and strain-hardening cement-based composite (SHCC) in conditions of hot-weather casting. In *Proceedings of the 10th International Conference on Mechanics and Physics of Creep, Shrinkage, and Durability of Concrete and Concrete Structures*, Vienna, Austria, 1504–1513. doi: 10.1061/9780784479346.176

Shiotani, T. and Aggelis, D.G. (2009). Wave propagation in cementitious material containing artificial distributed damage. *Materials and Structures, 42(3)*, 377–384. doi: 10.1617/s11527-008-9388-4

Yim, H.J., Kwak H.G. and Kim J.H. (2012). Wave attenuation measurement technique for nondestructive evaluation of concrete. *Nondestructive Testing and Evaluation, 27(1)*, 81-94. doi: 10.1080/10589759.2011.606319